Full-duplex Self-backhauling for Small-cell 5G Networks

Renaud-Alexandre Pitaval, Olav Tirkkonen, Risto Wichman; Aalto University, Espoo, Finland

Kari Pajukoski, Eeva Lähetkangas, Esa Tiirola; Nokia, Oulu, Finland

Abstract

We consider in-band self-backhauling for small cell 5G systems. In-band self-backhauling enables efficient usage of frequency resources, and when coupled with a flexible frame format, efficient Time Division Duplexing of uplink, downlink and backhaul transmissions. Self-backhauling is particularly efficient when coupled with full-duplex (FD) relaying. Antenna design, as well as cancelation in radio frequency and digital domains at a FD relay enables reuse of the same resources for backhaul and access hops. The use of radio resources in the self-backhauling and access hops can be coordinated to maximize end-to-end performance. We evaluate FD in-band self-backhauling in indoor 5G scenarios, targeting mobile broadband and ultrareliable communication use cases. Self-backhauling shows considerable promise for reaching 5G targets in these scenarios.

Introduction

Ongoing discussions on fifth generation (5G) radio access technology target up to 10 000 times increase in the total mobile broadband traffic in the 2020s, as compared to 2010. 5G will provide a ten-fold improvement of the user experience over 4G in terms of peak data rates and a noticeable reduction in terms of latency [1]. Traffic forecasts [2] predict that within the 5G timeframe, mobile video is likely to remain the most capacity-consuming traffic type, although considerable increase in volume for other types of traffic, such as Device-to-Device (D2D) and Machine-to-Machine (M2M) communication, as well as cloud-based usage of wireless devices is also foreseen. Designing solutions for the ensuing capacity crunch is the main objective of Mobile Broadband (MBB) access in 5G systems.

Requirements for higher capacity can be met by boosting the physical layer efficiency, using more spectrum, and by increasing the number of cells. For 5G, small cell deployments are of considerable interest. Decreasing cell size imposes high demands on the backhaul (BH) network connecting the increasing number of access points (AP) to a controlling node, to each other, and to external networks. In-band self-backhauling is an important enabler for cost-efficient transceiver design in an environment with scarce frequency resources. By defining a common radio interface that applies to all enhanced small cell traffic types – access links in uplink (UL) and downlink (DL), backhaul and D2D/M2M links, all controlled by the same network, no static frequency allocations would be required for different link types and the use of frequency resources would be optimized. Combining wireless in-band self-backhauling with dense small cell deployment is an important optimization goal in 5G physical layer design. Self-backhauling networks have also the advantage of low cost, and "plug-and-play" installation. Support of self-backhauling and multi-hop communication, however, imposes strict latency demands to 5G air interface.

Time division duplexing (TDD) is attractive when considering small cell communication with demands on high spectrum allocation flexibility and tight 5G -related cost efficiency requirements. TDD can be efficiently utilized to create flexible

Electronic postprint. DOI of published version: 10.1109/MWC.2015.7306541

resource partitioning between different link types and link directions, leading to efficient spectrum utilization. Also, the amount of available unpaired TDD spectrum is larger compared to the amount of paired spectrum. The costs of radio frequency components are low in TDD transceivers, because a duplexer filter is not needed and requirements of power amplifier can be relaxed, because the harmonics in the transmission do not overlap with the reception. Reciprocity can be utilized to avoid feeding back channel state information.

A flexible subframe structure for a 5G small cell TDD system was presented in [3] and is illustrated in Figure 1. A bi-directional L1/L2 control signal part is embedded to the beginning of each subframe and time-separated from a data plane containing data transmissions and higher layer signaling for either transmission or reception. TX and RX control is symmetrical to enable link-independent air interface – the same transmission subframe is used in uplink, downlink and in backhaul and access links. With self-backhauling and multi-hop, control information needs to be signaled not only between access nodes and terminals but also among the access nodes in the self-backhauling chain. Since in half-duplex communication, transmission and reception cannot be done simultaneously, a TDD problem arises where two nodes with the same TX/RX timing, cannot communicate with each other. To enable bi-directional communication in a TDD environment where all nodes are able to listen to each other, TX/RX patterns and pattern groups [4] can be utilized. In a flexible frame structure according to Figure 1, the Tx and Rx parts of the control plane, and the communication direction in the data plane would thus switch accordingly, on a per node basis. If self-backhauling nodes operate in full-duplex mode, i.e., they are capable of transmitting and receiving simultaneously in the same resource block, problems related to control signal communication restrictions are mitigated. To reach 5G targets on 1ms end-to-end latency in a multihop system, potentially with a Hybrid-ARQ (HARQ) retransmission protocol, the subframe has to be short. A subframe of 0.25ms is considered feasible in terms of control overhead in local area networks [3]. Time-multiplexed control and data planes enable the receiver to process its dedicated control information while transmitting/receiving data, which further reduces latency. The time-multiplexed structure also reduces energy consumption, because receivers do not need to receive and buffer data that is not targeted to them. Note that this is different from LTE, where control plane is multiplexed in time and frequency and receivers have to detect both data and control planes [5].

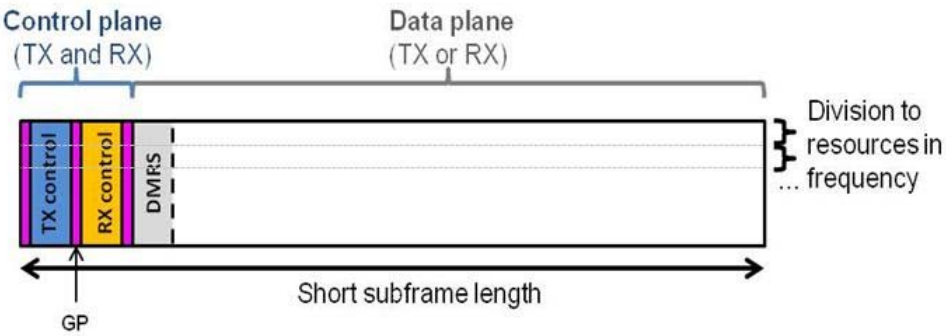

Figure 1. TDD optimized subframe structure.

Another aspect of prospective 5G networks is related to Ultra-Reliable Communication (URC) [6], where high reliability and low latency communication is required, primarily for machine type communication. URC is a key enabler for enhanced wireless automation in e.g. factory environments. To replace wires in factories, near-real time highly reliable wireless communication technologies are needed. Wireless communication provides clear advantages for flexible realization of wireless automation; ease of deployment, mobility, and scalability. Despite these benefits, compromised reliability and low capacity [7] have kept wireless solutions in a marginal role. This will change in 5G, with natively designed support for URC. Both cellular and D2D/M2M communications are foreseen in this context.

To increase the reliability of wireless transmission, one has to control excessive interference, and cope with unpredictable variations in communication channels. In a cellular network, access to the wireless medium is tightly controlled. This gives an edge to cellular over ad hoc networks which utilize license exempt frequencies. To achieve reliability in time-varying communication channels, either very rapid feedback, or overprovisioning of resources is required. A high reliability transmission requires more bandwidth than a low reliability transmission. Ultimately, in URC one is interested in a delay-limited outage capacity. For factory automation, this calls for high capacity indoor cellular networks, where capacity can be traded for reliability.

For self-backhauling with controlled reliability, we consider Decode-and-Forward (DF) relaying. In DF-multihop networks, end-to-end throughput decreases rapidly when the number of hops is increasing due to half-duplex losses. Making relays capable of full-duplex forwarding, throughput can be significantly increased, if self-interference can be canceled [8]. In practice, full-duplex devices with compact form factors suffer from self-interference caused by the coupling of the transmitted signal to the receiver chain, which decreases the gains from the full-duplex operation.

In this paper, we discuss in-band self-backhauling for dense indoor 5G deployments. A new category of low-cost Relaying-APs (R-APs) are considered for 5G small-cell networks. These operate in a TDD fashion, and serve as APs towards clients, while relaying traffic between fully equipped APs (F-APs) and client devices. Both full-duplex and half-duplex operation will be addressed. Mechanisms for canceling self-interference in full-duplex relays are considered to set realistic performance limits for full-duplex relays. Despite using projected state-of-the-art technologies, not all self-interference can be canceled. The residual self-interference may be on the level of other interference in the network, e.g., in a two-hop self-backhauling, to the interference from the source transmission to the destination. To balance the self-interference against other interference, link adaptation and Radio Resource Management (RRM) techniques can be used. Power control, resource allocation and Multiple-Input-Multiple-Output (MIMO) techniques can be used to mitigate interference. This can be with or without coordination between the backhaul and access links. Tight coordination enabled by RRM signaling provides significant gains for self-backhauling systems.

Assuming a reasonable residual self-interference level, achievable with state-of-the art technologies, a multi-hop network with full duplex relays and RRM coordinating backhaul and access links significantly outperforms a network with half-duplex relays, and a conventional single-hop cellular network.

Self-backhauling Networks with Full-duplex Relays

To enable optimization of frequency and time usage in a self-backhauling 5G network, we consider APs that act as in-band relays. Differing from conventional relaying in cellular systems, where carefully placed relay nodes mitigate coverage holes, with self-backhauling small cells a dense deployment of relatively cheap relay nodes may be considered. This leads to diversity gains from selecting the relay routes. In [9] and references therein it was observed that significant gains are achieved by densifying the network of relay nodes. Also, it was found that most of the gain from in-band self-backhauling can be achieved with one backhaul hop, and that using Full Duplexing (FD) in the relaying APs as opposed to Half Duplexing (HD) provides significant gains.

The major cost increase in the discussed solution is the cost of deploying the dense network of R-APs. Accordingly, these should be relatively simple devices. We consider R-APs that operate as physical layer forwarders, which decode the messages to prevent error propagation, and to enable interference cancelation, but do not perform any L2 functionalities independently of the F-APs. We assume that the R-APs serve at most one user at the time, and do not perform buffering or queue management.

In Figure 2, radio channels, communication channels and RRM opportunities are depicted for a two-hop full-duplex self-backhauling flow. In Figure 2 a), the radio channels between the source, the relay and destination are depicted. There is a wanted signal channel for both hops, and a direct channel from the source to the destination. In addition, for full-duplex operation, there is a self-interference channel. Figure 2 b) depicts the assumed L1/L2 control signaling channels. For these, the control-part of the subframe in Figure 1 is used. Scheduling and link adaptation information is transmitted by the F-AP, and channel state information such as Channel Quality Indication (CQI) and Precoder Matrix Indication (PMI) is transmitted from the UE and the R-AP to the F-AP. The control connection between the UE and the F-AP can be realized either as a direct transmission over the air, or as a transmission relayed by the R-AP. In Figure 2 c), the data plane communication in a self-backhauling configuration is depicted. A full-duplex R-AP simultaneously receives from the F-AP and transmits to the UE, or vice versa. The DF functionality is realized on a sub-frame basis. If transmissions within a subframe depicted in Figure 1 are segmented to coding blocks in the time domain, pipeline processing is possible. Then, a transmission received by a R-AP in subframe *n* would be forwarded in subframe *n*+1, if processing time is minimized. It is worth noting that in the discussed FD self-backhauling scheme, only the R-APs need to be FD capable. The UEs, and F-APs, may operate in a TDD fashion. Also, the R-APs would also follow a TDD principle between uplink and downlink flows. In contrast to F-APs and UEs, the traffic flow in R-AP is inherently symmetric. This architecture makes full use of full-duplex technology.

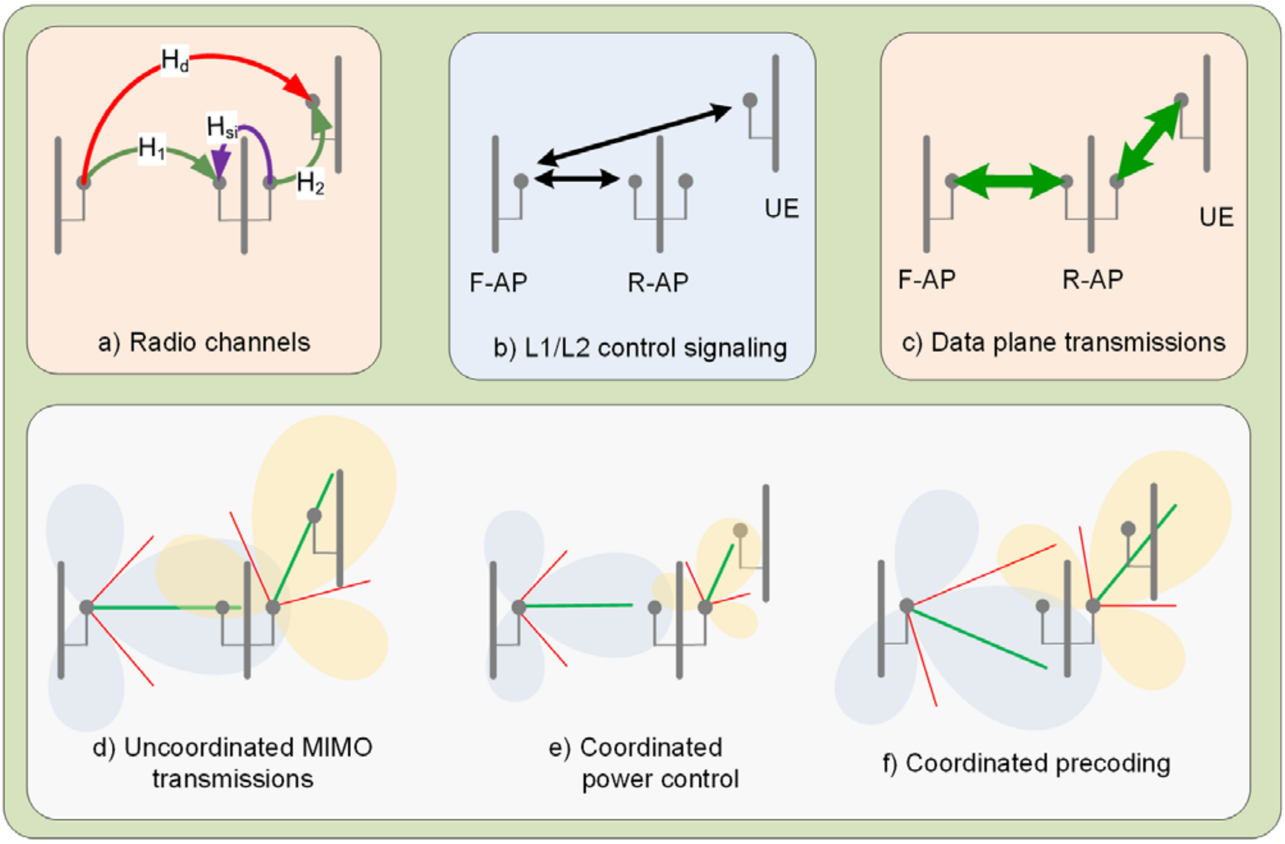

Figure 2. Two-hop full-duplex self-backhauling.

The grand challenge in full-duplex transceivers is the cancellation of self-interference, which is caused by the leakage of the transmitted signal to the receiver chain. A straightforward way to reduce self-interference is to increase the distance between the transmitter and receiver antennas, i.e. decrease the gain of $\boldsymbol{H}_{si}$ in Figure 2 a). This is used in broadcast networks but it is not possible in small cells. On the other hand, employing the same antenna to transmit and receive together with a circulator or other active analog cancellation techniques, provides limited isolation. In addition, RF cancellation techniques are typically narrow band. However, even with compact relays it is possible to achieve wideband antenna isolation of the order of 55 dB [10] on 130 MHz band at 2.6 GHz carrier frequency, when the spatial distance between the antennas is only few centimeters. Adding analog cancellation improves the attenuation of self-interference up to 75 dB, but in a 10 MHz band only. Total interference cancellation levels of the order of 70-100 dB have been reported [11].

Figure 3 depicts three complementary techniques to mitigate self-interference in full-duplex R-APs: spatial isolation, RF cancellation and digital cancellation. First, spatial isolation and RF cancellation should attenuate the self-interference so that the remaining interference signal is within the dynamic range of analog-to-digital converter to enable its digital cancellation. The digital baseband transmitted signal is known, and it can be subtracted from the received signal once $\boldsymbol{H}_{si}$ in Figure 2 a) has been estimated. The efficiency of linear interference cancellation is limited due to RF imperfections and channel estimation errors, as the unknown part of the transmitted signal cannot be subtracted in digital baseband. Modeling nonlinear effects due to RF imperfections and modifying the subtracted self-interference signal accordingly, residual self-interference can be pushed down to noise floor after digital cancellation [12]. The effects of RF imperfections are typically modeled by error vector magnitude (EVM) and their maximum power levels in, e.g. LTE, are required to be between -22 dB and – 15 dB depending on modulation [5]. Cancellation of self-interference in FD R-AP consumes additional power, but the increase in hardware cost is not expected to be more than a factor of two.

Here we model the self-interference channel by a random matrix $\boldsymbol{H}_{si}$.. The residual self-interference signal is given by $\boldsymbol{H}_{si}\,\boldsymbol{e}$, where $\boldsymbol{e}$ is the distorted part of the transmitted signal remaining after cancellation. The mean attenuation of the self-interference achieved by spatial isolation, RF cancellation and subtraction of the interference in digital baseband is embedded in the power of $\boldsymbol{H}_{si}\,\boldsymbol{e}$. The residual self-interference term acts like colored noise, and transmit and receive precoders $\boldsymbol{W}_{tx}$ and $\boldsymbol{W}_{rx}$ in Figure 3, and/or their powers, can be optimized to maximize the mutual information [13]. When the number of antennas in F-AP and R-AP is larger or equal to twice the transmission rank, $\boldsymbol{W}_{tx}$ and $\boldsymbol{W}_{rx}$ can be designed such that R-AP transmits and receives in orthogonal subspaces and self-interference is completely removed.

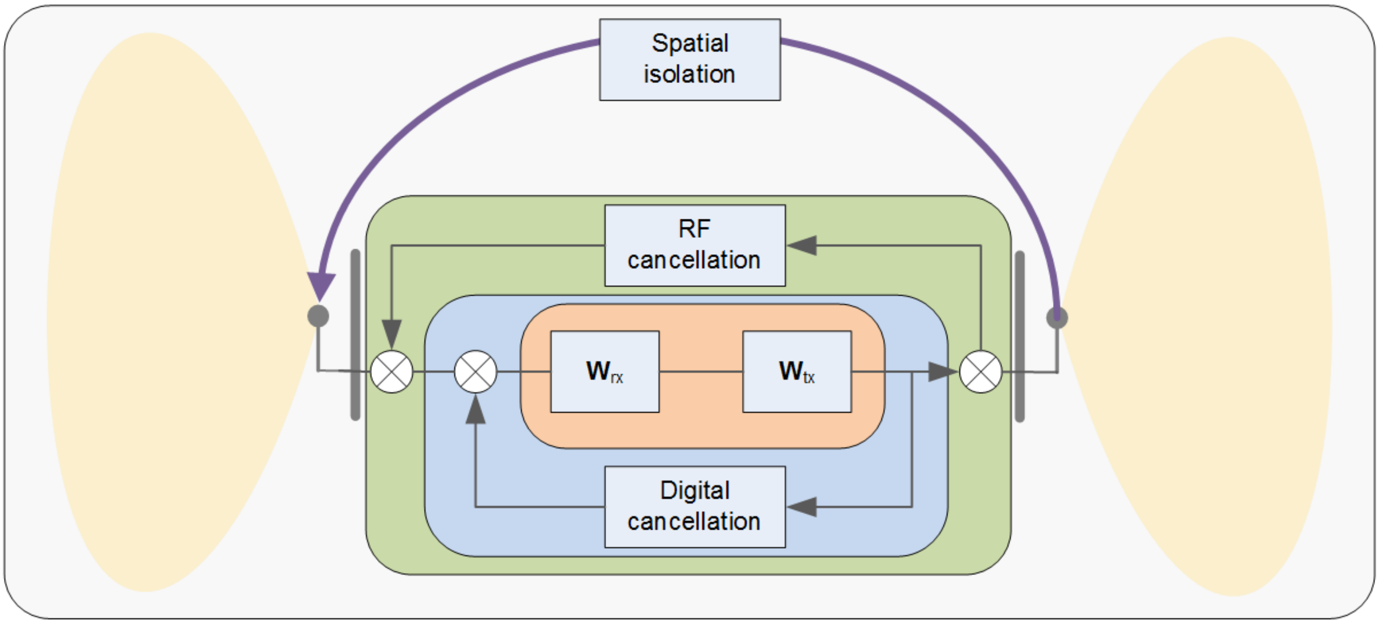

Figure 3. Self-interference cancellation mechanisms in a full-duplex relay.

Coordinated Interference Management Between Backhaul and Access Hops

In a cellular system, RRM is used to control interference. In a multi-hop self-backhauling scenario, there is *intra-flow interference* in addition to conventional inter-cell interference. Significant gains can be achieved by *coordinated RRM* of a multihop flow. For a two-hop flow of Figure 2 c), this would mean coordinating the data plane transmissions on the self-backhauling and access hop of a flow. This would be performed by the F-AP, based on information gathered over the L1/L2 control channels from the R-AP and UE. Coordination in RRM can be related to many PHY and MAC layer functions, such as power control (PC), resource allocation, and MIMO precoding.

If the relays operate in half-duplex Decode-and-Forward (DF) manner, and transmission and reception at a node is Time Division Duplexed (TDD), resource allocation can be optimized in time domain. The pattern of transmission and reception in the data plane for the two hops can be selected to guarantee optimal usage of the radio resources. Without TDD optimization of a HD two-hop flow, the source and the relay would be transmitting only 50% of the time. Accordingly, with ideal Interference Cancelation (IC), up to 100% gain could be expected from an ideal full-duplex transmission.

The efficiency of full-duplex relaying is compromised by intra-flow interference, as depicted in Figure 2 a). With FD, the performance limitation in the network is primarily this intra-flow interference rather than inter-cell interference. There are two bottlenecks in FD relaying preventing ideal gain. First, the residual self-interference (SI) at the relay, after the interference mitigation and cancelation in the relay, is of prime importance. Second, the direct link between the source and destination also creates interference, but attenuated by path loss. The dominant bottleneck depends on the full duplexing implementation in the R-AP, and system characteristics. In the indoor scenario investigated here, self-interference at R-AP is the dominant bottleneck with SI attenuation of 80dBs, whereas with 100dB SI attenuation, the direct link becomes dominant.

In FD relaying with uncoordinated RRM, depicted in Figure 2 d), the self-backhauling link is separately optimized from the access link. The R-AP may optimize its transmit power and MIMO precoding to optimize its reception. Coordinating the RRM between the two hops provides significant gain potential to trade off the two bottlenecks of a flow. The simplest coordination of the transmission in the two hops would be coordinated power control (PC), depicted in Figure 2 e). Depending on which of the interferences is the dominant bottleneck, one of the transmitters would reduce its power. Uncoordinated PC to mitigate self-interference in the R-AP was considered in [14], whereas coordinated PC was addressed in [9]. A further dimension of coordination is in MIMO precoding depicted in Figure 2 f). The spatial directions of the two transmissions, i.e., the precoders, can be jointly optimized to mitigate interference as in [13] which assumed joint power budget for R-APs and F-AP in order to formulate the optimization problem. Here we assume that maximum transmit powers of different nodes are only limited by hardware constraints without constraining the total transmit power in the network.

An information segment transmitted from the source to the R-AP, and then from the R-AP to the destination is received twice at the destination: first, as a weak transmission over the direct link $\boldsymbol{H}_d$, then as a strong transmission from the R-AP. If the first signal is ignored, it simply causes interference at the destination. If the destination is capable of canceling the interference from the direct link, or to combine the weak signal received over $\boldsymbol{H}_d$ with a strong forwarded transmission, performance can be improved. We consider two strategies for direct link interference mitigation at the destination, sequential combination or time-reversed cancelation. In sequential *direct link signal combination*, the destination estimates a symbol sequentially first from the direct link transmission then combines it with the symbol estimation from the second-hop transmission. In time-reversed *direct link IC*, perfect IC is obtained by performing symbol detection only after a frame of symbols, consisting of multiple sub-frames, is received. When transmitting a frame, the source does not transmit in the last sub-frame. The destination thus receives the last subframe without direct link interference, and can decode this sub-frame with better SINR. After decoding the last subframe, the interference from the direct transmission can be sequentially canceled in a time-reversed manner. This strategy incurs additional delay, and a minor rate loss depending on the size of the frame. Combining the decoding of m slots, with a corresponding increase in delay, the rate loss is $(m-1)/m$. In simulations, the frame consists of 15 slots, and the rate loss is 14/15.

Simulation Results

Simulation Assumptions

For mobile broadband services, the highest capacity requirements are expected in indoor locations, and URC networks for factory automation are also predominantly indoors. To address the potential of full-duplex multi-hop relaying we thus consider indoor small-cell networks consisting of F-APs, which have a wired connection to the internet, and R-APs, that are connected by self-backhaul to an F-AP. The APs collaborate to serve a population of users, or machines.

To address 5G objectives both for MBB and URC, we perform simulations in two scenarios. For MBB, we consider an indoor local area deployment in a dense urban environment. A self-backhauling network is deployed in a Manhattan grid of multi-floor buildings. The simulation model is discussed in [9], and is based on Winner path loss models [15]. The buildings are according to the Indoor-office A1-model of [15]. The basic unit of a building is a 10x10 meter room, and there are two 5m-wide corridors between rows of rooms. The size of the building is 50x100m consisting of 40 rooms per floor. There are three floors in each building, and four F-APs per floor located in the corridors. The two F-APs in the same corridor are 50m apart. One R-AP is placed in a random position in each room. There are four buildings in the model, placed in a Manhattan grid 20m apart from each other. Wrap-around boundary conditions are applied in the two horizontal directions. Following the Indoor-to-outdoor model A2 in [15], the loss in the outer walls of the buildings is between 14 and 29dB, depending on the direction. For URC, we consider a factory scenario consisting of a Manhattan grid of one-floor factories. Each factory has the same size, and the same placement of F-APs and R-APs as the buildings in the MBB scenario, except that there are no inner walls. In the factory, non-line-of sight is assumed, with path loss exponent 3. Some of the most important simulation parameters can be found in Table I.

We consider downlink flows. Each R-AP is associated with a F-AP with the smallest direct link pathloss, thereby dividing the network into cells. Cell selection for the UEs is similarly based on average path loss. UEs are distributed uniformly in the buildings. It is assumed that there is an active UE in 20% of the cells, and in each cell there is only one active UE. The MIMO channels between the transmitters and receivers, as well as between the transmitters and all interference victims in the network, are modeled, taking distance dependent path loss, shadow fading and Rayleigh-distributed uncorrelated fast fading into account. After RRM, the Signal-to-Interference-plus-Noise Ratios (SINRs) of the receivers are calculated, for each MIMO layer transmitted.

For MBB, we are interested in high data rates, and rely on end-to-end HARQ for reliability. This is realized by applying a margin when controlling the SINR of the self-backhauling hop. Transmission packets to the users are transmitted in subframes with segments of equal size, and the flow is operating for tens of subframes. Physical layer throughput is modeled by using Adaptive Modulation and Coding with a throughput close to Shannon's law, with an implementation margin of 2 dB. The largest SINR allowed by the RF impairments is 25dB, which sets the highest transmission rate in the system. Bandwidth efficiency is 90%, as in LTE, which decreases achievable rates in linear manner.

For URC, HARQ is not applied against SINR variations arising from imperfect precoding, and variations in interference. Note that the self-interference experienced in the R-AP is a random variable, which causes fading in the F-AP to R-AP communication in this scenario. In addition, mobility causes errors in precoder selection and CQI. For each flow towards a user, we consider an implementation limited outage capacity. A rate that is achievable with 99,9% reliability over the self-interference and mobility-induced fading is considered. In the simulation, we consider an environment, where machines are moving with a 20 km/h velocity. With a 0.25 ms subframe, and two-hop communication, a CQI delay of 0.5 ms may be expected. Accordingly, measured channels and channel realizations at the time of transmission are 99% correlated. We use an eigenbeam transmitter and receiver, with separate coding per MIMO layer. To decrease outage probability, a margin is applied to measured CQIs. With a first order approximation to estimate the statistics of realized channels, a 12dB margin is sufficient to guarantee target reliability. For URC, short subframes are highly important to increase the reliability of feedback information, especially CQI.

For self-interference cancelation at the FD R-AP, we consider two values, 80dB and 100dB. The former may be realistic in future wide band transmissions as foreseen in MBB, and the latter may be realistic in narrower bands [10][11], pertinent for URC. Coordinated RRM over the two hops is compared with uncoordinated RRM, based on precoder and power control. For half-duplexing transmission, time domain resource optimization is performed. Direct link IC is used based on a time-reversal strategy, with a frame consisting of 15 subframes.

The statistics in the simulations are collected over 1000 network instances. In the simulations, cross-interference between the cells is taken into account. Detailed system simulation parameters are shown in Table 1.

Table 1. System Level Simulation Parameters

F-APs in the network	MBB:48 URC: 16
R-APs in the network	MBB:480 URC: 160
Floors in the buildings	MBB: 3 URC: 1
Boundary conditions	wrap-around in XY-direction
Maximum Tx power (F-APs and R-APs)	24 dBm
Carrier frequency	3.6 GHz
Bandwidth	MBB: 100 MHz URC: 5 MHz
Bandwidth efficiency	0.9
MIMO-configuration	1x1, 2x2, 4x4
Inner wall loss	MBB: 5 dB URC: 0 dB

Performance Results

Throughput performance in the MBB scenario can be found in Figure 4. The Cumulative Distribution function (CDF) of user throughput is depicted. In addition, relative gains of different strategies over direct transmission are given, at the 5% point of the user throughput. This reflects the service offered to cell-edge users.

With 80 dB SI cancelation, we see a clear gain from coordinated RRM with FD. If RRM is enabled to choose between HD and FD, some additional gains would be realized. Direct link cancelation/combination provides little gain with coordinated RRM. However, with hypothetical 100dB SI cancelation, when the direct link interference is the bottleneck, direct link IC provides noticeable gains. Sequential direct link combination provides worse performance, and is not depicted.

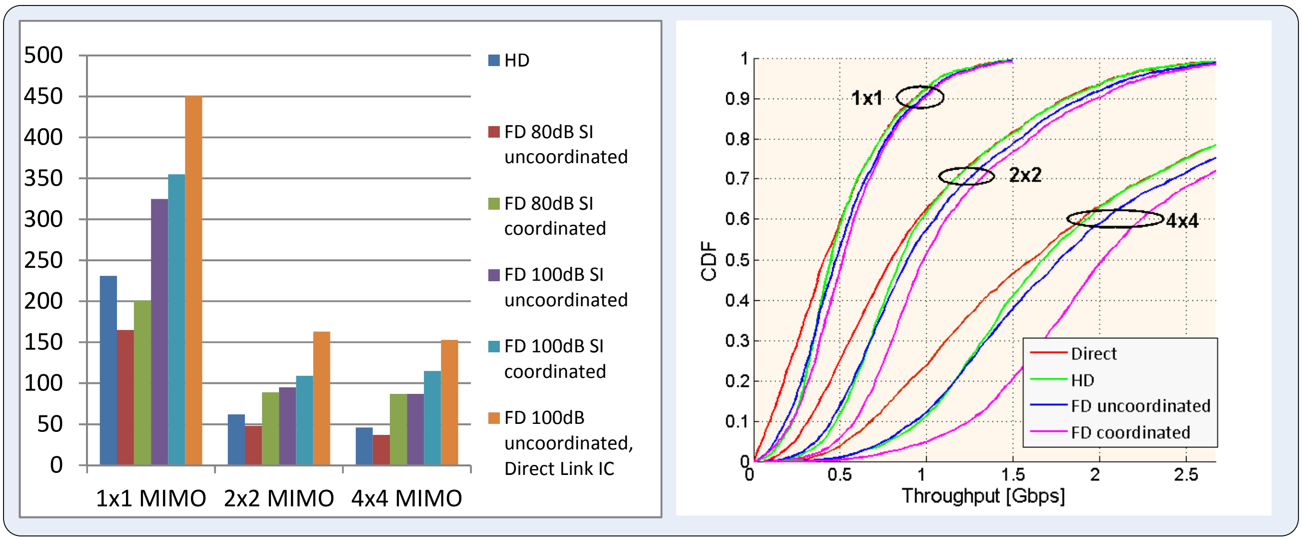

Figure 4. MBB scenario: Left: Throughput at 5% of user throughput CDF, gain [%] relative to direct communication with F-AP only, i.e. (MultiHop- Direct)/Direct in %. Right: CDF of user throughput [Gbps], 1x1, 2x2 and 4x4 MIMO. Self-interference cancelation 80 dB at R-AP.

Outage capacity performance in the URC scenario can be found in Figure 5. The CDF of the rate that a receiver can enjoy with 99,9% probability at a given location is depicted. In addition, relative gains over direct transmission are given, at the 5% point of the user outage capacity CDF. These represent the gains in the rate that can be offered to 95% of the locations in the factory, with 99,9% of reliability against changing fading conditions. With 100dB SI cancelation, remarkable gains from relaying, FD operation and direct link IC are observed. Due to the required reliability, the gains from routing diversity against shadow fading persist even with MIMO transmissions. This lays the foundation for the other gain mechanisms.

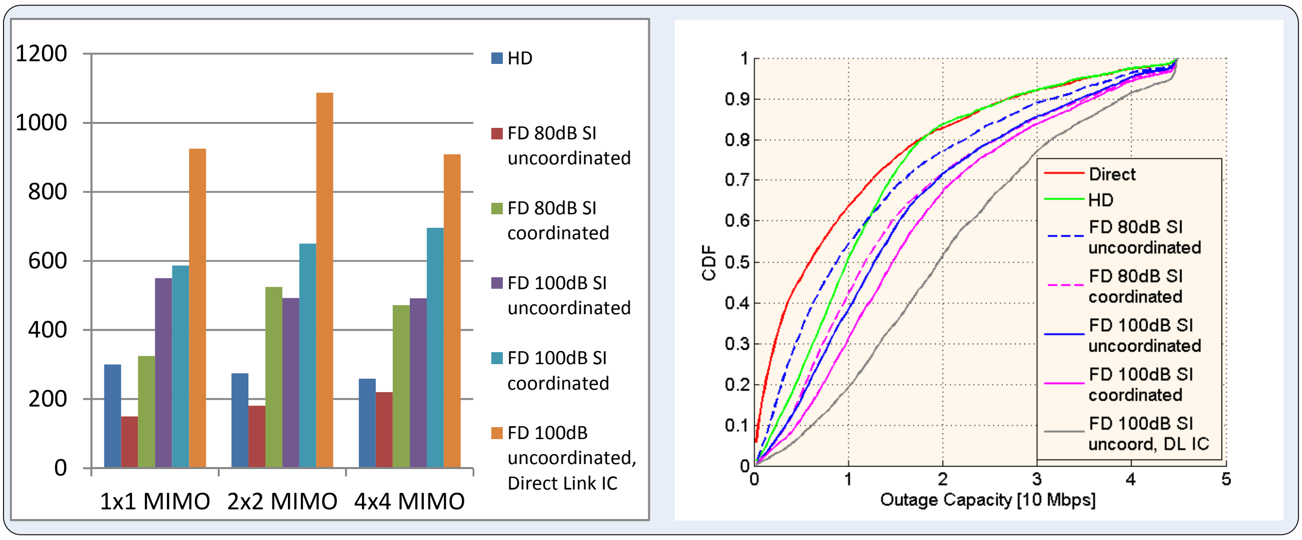

Figure 5. URC scenario: 0.1% Outage Capacity. Left: Outage capacity at 5% of CDF, gain [%] relative to direct communication with F-AP only. Right: CDF of outage capacity [10 Mbps], 2x2 MIMO.

Conclusion

We considered in-band backhauling for 5G small-cell networks. A flexible frame format enables effective use of time and frequency resources for both uplink, downlink and backhaul transmissions. Relay nodes are densely deployed in the network to provide routing diversity for two-hop transmissions. A two-hop full duplex self-backhauling flow has two possible bottlenecks, either the self-interference in the FD relay, or the interference from the direct transmission to the destination. The dominant bottleneck depends on the link distances, and the efficiency of self-interference cancelation at the FD relay. Coordinated RRM between the self-backhauling and access hops proved to be efficient. The drawback of the discussed solution is in increased infrastructure costs due to the numerous relay nodes. The price of these can, however, be kept low by restricting the relays to operate as forwarders of coded bit transmissions, without L2 functionalities. We conclude that FD self-backhauling is a valuable technology component when striving for the gigabit experience in MBB; and for the ultra-reliability in URC.

Acknowledgement

The authors would like to thank Mr. Karol Schober and Mr. Ilkka Harjula for participating in the development of the simulator.

References

[1] Nokia whitepaper: “FutureWorks – Looking ahead to 5G: Building a virtual zero latency gigabit experience”, available at http://networks.nokia.com/sites/default/files/document/5g_white_paper_0.pdf.

[2] Cisco, “Cisco visual networking index: Global mobile data traffic forecast update, 2011-2016,” White paper, 2012.

[3] P. Mogensen, K. Pajukoski, E. Tiirola, J. Vihriälä, E. Lähetkangas, G. Berardinelli et al., “Centimeter-wave concept for 5G ultra-dense small cells”, IEEE VTC 2014 Spring, MWC2020 workshop, May, 2014.

[4] E. Tiirola, B. Raaf, E. Lähetkangas, I. Harjula, K. Pajukoski, ” On the Design of Discovery Patterns for Half-Duplex TDD Nodes Operating in Frame-Based Systems”, Future Network and Mobile Summit, 2013, pp.1-9, July 2013.

[5] H. Holma, A. Toskala (eds.), “LTE for UMTS: OFDMA and SC-FDMA based radio access,” Wiley, 2009.

[6] P. Popovski, ”Ultra-Reliable Communication in 5G Wireless Systems,” 5GU conference, 6 pp., Nov. 2014.

[7] G. Gaderer, P. Loschmidt, A. Mahmood, ”A novel Approach for Flexible Wireless Automation in Real-Time Environments,” IEEE Int. Workshop on Factory Communication Systems, pp. 81-84, 2008.

[8] H. Ju, S. Lim; D. Kim, H.V. Poor, D. Hong, "Full Duplexity in Beamforming-Based Multi-Hop Relay Networks," IEEE Journal Select. Areas Commun., vol.30, no.8, pp.1554-1565, Sep. 2012.

[9] I. Harjula, R. Wichman, K. Pajukoski, E. Lähetkangas, E. Tiirola, O. Tirkkonen, ” Full Duplex Relaying for Local Area,” IEEE PIMRC 2013.

[10] S. Venkatasubramanian, L. Li, C. Icheln, F. Ferrero, C. Luxey, K. Haneda, “Impact of Neutralization on Isolation in Co-Planar and Back-to-Back Antennas,” Eur. Conf. on Antennas and Propagation, Apr. 2015.

[11] A. Sabharwal, P. Schniter, D. Guo, D. Bliss, S. Rangarajan, and R. Wichman, “In-band full-duplex wireless: Challenges and opportunities,” IEEE Journal Selected Areas Commun., vol. 32, no. 9, pp. 1637–1652, Oct. 2014.

[12] D. Bharadia, E. McMilin, S. Katti, “Full-duplex Radios,”, ACM SIGCOMM, Aug. 2013.

[13] D.W.K. Ng, E.S. Lo, R. Schober, "Dynamic Resource Allocation in MIMO-OFDMA Systems with Full-Duplex and Hybrid Relaying," IEEE Trans. Commun., vol.60, no.5, pp.1291,1304, May 2012.

[14] T. Riihonen, S. Werner, R. Wichman, Hybrid Full-Duplex/Half-Duplex Relaying with Transmit Power Adaptation, IEEE Trans. Wireless Commun., vol 10, no. 9, Sep. 2011.

[15] P. Kyösti & al. “Winner II channel models,” Tech. Rep. D1.1.2 V1.2, 2007, available: http://www.ist-winner.org.